Lysosomal cathepsin B participates in the podosome-mediated extracellular matrix degradation and invasion via secreted lysosomes in v-Src fibroblasts

Chun Tu[1,5], **Cesar F. Ortega-Cava**[1,5], **Gengsheng Chen**[5], **Norvin D. Fernandes**[6], **Dora Cavallo-Medved**[4], **Bonnie F. Sloane**[4], **Vimla Band**[3,5], and **Hamid Band**[1,2,5,*]

[1]Eppley Institute for Research in Cancer and Allied Diseases, and UNMC-Eppley Cancer Center, University of Nebraska Medical Center, Omaha, NE 68198-6805

[2]Department of Biochemistry and Molecular Biology, College of Medicine, University of Nebraska Medical Center, Omaha, NE 68198-5805

[3]Department of Genetics, Cell Biology and Anatomy, College of Medicine, and UNMC-Eppley Cancer Center, University of Nebraska Medical Center, Omaha, NE 68198-5805

[4]Department of Pharmacology and Barbara Ann Karmanos Cancer Institute, Wayne State University School of Medicine, Detroit, MI

[5]This work was initiated and substantially performed while the authors were at the Divisions of Molecular Oncology and Cancer Biology, Evanston Northwestern Healthcare Research Institute, Department of Medicine, Feinberg School of Medicine; Robert H. Lurie Comprehensive Cancer Center, and Department of Biochemistry, Molecular Biology and Cell Biology, Northwestern University, Evanston, IL 60201

[6]Dana-Farber Cancer Institute, Boston, Massachusetts

Abstract

Podosomes mediate cell migration and invasion by coordinating the reorganization of actin cytoskeleton and focal matrix degradation. Matrix metalloproteases and serine proteases have been found to function at podosomes. The lysosomal cysteine cathepsins, a third major class of matrix-degrading enzymes involved in tumor invasion and tissue remodeling, have yet to be linked to podosome with the exception of cathepsin K in osteoclasts. Using inhibitors and shRNA-mediated depletion, we show that cathepsin B participate in podosomes-mediated focal matrix degradation and invasion in v-Src transformed fibroblasts., We observed that lysosomal marker LAMP-1 localized at the center of podosome rosettes protruding into extracellular matrix using confocal microscopy. Time-lapse live-cell imaging revealed that lysosomal vesicles moved to and fused with podosomes. Disruption of lysosomal pH gradient with Bafilomycin A1, chloroquine or ammonium chloride greatly enhanced the formation of podosomes and increased the matrix degradation. Live cell imaging showed that actin-structures, induced shortly after Bafilomycin A1 treatment, were closely associated with lysosomes. Overall, our results suggest that cathepsin B, delivered by lysosomal vesicles, are involved in the matrix degradtion of podosomes.

---

*To whom correspondence should be addressed at: Eppley Institute 986805 Nebraska Medical Center Omaha, NE 68198-6805 Phone: 402-559-8572 FAX: 402-559-2823 hband@unmc.edu.
Current Address: GC: Coskata Energy Inc., Warrenville, Illinois; NDF

INTRODUCTION

Podosomes, originally identified in normal cells capable of moving through tissue boundaries (1), are dot- or ring-like actin-rich structures localized at the ventral side of cells in contact with the extracellular matrix (ECM). Invadopodia, related structures in tumor cells, were first described in oncogenic Src-transformed fibroblasts (2) and subsequently observed in many invasive cancer cells (3,4). Since podosomes and invadopodia exhibit a similar molecular makeup and mediate similar functions (5–7), they are likely to represent variants of a related basic structure. For simplicity, we use the term podosomes to describe these matrix-digesting actin rich-structures in this study.

Podosomes are sites of active actin reorganization where many regulators of actin cytoskeleton, such as N-WASP (8), Arp2/3 complex, cdc42, Rho (9), cortactin (10), and Nck1 (11) localize. Additionally, members of Src family kinases (12) and their substrates such as Tks5/Fish (13) are essential components of podosomes. When the formation of podosomes is perturbed by depriving or functionally interfering with these podosome components, the abilities of cells to migrate and invade are invariably impaired (8–11,13).

Another prominent feature of podosomes is focal proteolysis of ECM, which enables cells to migrate and invade by creating tracks for cells to migrate on. Three classes of matrix-digesting proteases have been implicated in the progression of tumor cells: matrix metalloproteases (MMPs)(14), serine proteases (15), and lysosomal cysteine cathepsins (16–19). Among them, multiple types of MMPs (7,20,21) and serine proteases (22–24) in podosome were shown to function at podosomes of many cells including cancer cells. In contrast, little is known about the role of cancer-related cathepsins such as cathepsin B in podosomes. The only cysteine cathepsin known to function in podosomes is cathepsin K (25), which specifically participate in bone matrix resorption in osteoclasts.

Evidence for a link between lysosomes and podosomes mainly comes from osteoclasts. The whole lysosomal compartment of differentiated bone-resorbing osteoclasts is targeted to the cell-matrix interface enclosed by a specialized podosome structure called sealing zone (26–29). Consequently, Late endosome/lysosomal membrane proteins, lysosomal proton pump vacuolar H^+-ATPase (29), and lysosomal enzymes (25) are found at podosomes of osteoclasts. Recent studies suggest that the lysosome-podosome connection are not limited to osteoclasts: lysosomal membrane proteins such as CD63 (30) and LYAAT (31) are localized at podosomes of HeLa cells and mouse fibroblasts; Src family kinases, both necessary and sufficient to induce podosome formation, are found in both lysosomes and at podosomes (31,32). Importantly, the lysosomal localization of the Src family kinase p61[hck] is required for podosome induction in NIH3T3 cells (31), suggesting a functional connection between them.

Based on these data, we speculate that lysosomal cysteine cathepsins may participate in matrix degradation by targeting of lysosomes to podosomes. To test this hypothesis, we first investigated the role of the lysosomal cysteine cathepsin B on podosome function in v-Src-transformed fibroblasts. Enzymatic inhibitors of cysteine cathepsins or shRNA-mediated depletion of cathepsins B reduced both the degradation of extracellular matrix and Matrigel invasion by v-Src-transformed cells. Furthermore, lysosomal marker lysosomal associated membrane protein-1 (LAMP-1) was localized at the center of podosome rosettes protruding into matrix-degradation areas. Live cell imaging showed that lysosomal vesicles moved to and fused with podosomes. Disruption of lysosome pH gradient promoted podosome formation and cathepsin B-dependent degradation of extracellular matrix. Taken together, our results suggest that lysosomes and lysosomal cystein cathepsin B are involved in podosome function.

MATERIALS AND METHODS

Biochemical reagents and antibodies

CA-074, CA-074Me, E64c and E64d were from Peptide International (Louisville, KY). GM6001, PP2, Bafilomycin A1 and cathepsin B detection kit were from Calbiochem (San Diego, CA). Lysotracker Red DND-99 and Mitotracker Red CMXRos were from Invitrogen (Eugene, OR). Cy3 labeling kit was from Amersham (Piscataway, NJ). The rabbit anti-cathepsin B antibody used here has been described previously (33). Anti-phosphotyrosine antibody 4G10 was a gift from Dr. Brian Druker (Oregon Health & Science University, Portland, OR). Anti-Cortactin antibody 4F11 was purchased from Upstate Biotechnology Inc. (Lake Placid, NY). Anti-mouse LAMP-1 antibody 1D4B was obtained from the NIH Developmental Studies Hybridoma Bank at the University of Iowa. Secondary antibodies were from Invitrogen (Eugene, OR).

DNA constructs

v-Src cDNA sequence was PCR-amplified from the pLNCX-v-Src plasmid (gift of Dr. Joan Brugge, Harvard Medical School), and the fragment was digested with Cla I and cloned into Hpa I site of the pMSCV-Hygro vector (Clontech, Mountain View, CA). CFP-β-actin construct pEX-EF1-Actin-b-CFP was purchased from ATCC)*Cell lines:* NIH3T3 cells (ATCC, Rockville, MD) were retrovirally transduced with MSCV-hygro vector or MSCV-hygro-v-Src and selected in 100 μg/ml hygromycin. All cell lines were maintained in Dulbecco's Modified Eagle's Medium (DMEM, Gibco, Carlsbad, CA) containing 5% fetal bovine serum (HyClone, Logan, UT), 2mM L-glutamine, and penicillin/streptomycin.

Extracellular matrix degradation assay

Cy3-gelatin-coated coverslips were prepared as described (Bowden et al., 2001) with certain modifications. Gelatin was labeled using a Cy3 labeling kit (Amersham, Piscataway, NJ) according to the manufacturer's instructions and dialyzed against PBS. Cy3-gelatin was coated onto glass coverslips and crosslinked with 0.5% glutaraldehyde in PBS for 30 minutes. Coated coverslips were then washed three times each with PBS and 50 mM glycine in PBS. Cells were cultured for various time points to allow ECM degradation, seen as focal loss of fluorescent signal ("holes") in the labeled gelatin layer.

Immunofluorescence microscopy on fixed cells

Cells grown on coverslips (VWR, Batavia, IL) were fixed in 3.5% paraformaldehyde (PFA) for 30 min at room temperature (RT), permeabilized in 0.5% Triton X-100/PBS, blocked with 2% BSA (Sigma, Saint Louis, MO) in PBS, and incubated with primary antibodies in 2% BSA/PBS. Bound primary antibodies were detected with Alexa 488- or Alexa 647-conjugated goat anti-mouse or goat anti-rabbit secondary antibodies (Invitrogen, Eugene, OR). Polymerized actin was visualized with Alexa 488- or Alexa 647-conjugated phalloidin (Molecular probes, Eugene, OR). Z-stack confocal fluorescence images were obtained with a LSM510 fluorescence confocal microscope (Carl Zeiss, Thornwood, NY) under a 63x oil immersion lens. Other confocal fluorescence images were observed with a Nikon Eclipse microscope (Melville, NY) under a 63x oil immersion lens. Images were processed using the Adobe Photoshop software (Adobe Systems). Areas of degradation were quantified by enumerating total pixels of digested gelatin areas using NIH Image J software[7]. Data were compiled from three independent experiments.

---

[7]http://rsb.info.nih.gov/ij

Time-lapse live cell Imaging

The v-Src transformed NIH3T3 cells were plated on glass bottom chamber slides (BD Bioscience, San Jose, CA) and transfected with CFP-β-actin using the Fugene 6 reagent (Roche Diagnostics, Indianapolis, IN) according to the manufacturer's instructions. Twenty-four hours after transfection, cells were placed on the stage of a LSM 510 fluorescence confocal microscope (Carl Zeiss, Thornwood, NY) and maintained at 37 °C in a CO_2-independent medium (Invitrogen, Eugene, OR) supplemented with 5% FCS. Cells were then loaded with either a cathepsin B selective substrate (crystal violet conjugated [RR] $_2$ from Calbiochem, San Diego, CA) or Lysotracker Red DND99 (Invitrogen, Eugene, OR). For Bafilomycin A1 experiments, cells were first loaded with lysosomal tracer for more than 15 minutes before adding 20 µM Bafilomycin A1 (Calbiochem, San Diego, CA). Images were collected with a 63x oil immersion objective lens. Data analysis was performed using LSM 510 software.

shRNA knockdown experiments

Lentiviral shRNA constructs against mouse cathepsins B were purchased from Open Biosystems Inc. (Huntsville, AL). These were transiently co-transfected with packaging plasmids pLP1, pLP2, and pLP/VSVG (Invitrogen, Carlsbad, CA) into 293FT packaging cells (Invitrogen, Carlsbad, CA) using the calcium phosphate precipitation method to generate lentiviral supernatants. The mouse cathepsin B specific shRNA sequences target against 5'-aggtgcaacaagagctgtgaa-3' and 5'-gacttacaaatcaggagtata-3'. The supernatants were used to infect the v-Src-transformed NIH3T3 cells followed by selection and maintenance in medium containing 5 µg/ml puromycin (Sigma, Saint Louis, MO) as described (38).

Matrigel invasion assay

Matrigel invasion chambers (Becton Dickinson Biosciences, Bedford, MA) were pre-hydrated for 3 hours with serum-free medium. Twenty-five thousand cells in 400 µl serum-free medium were placed in the top chambers and medium containing 5% FCS was placed in the bottom chambers. The chambers were incubated at 37 °C for 24 hours. Non-invading cells were removed from the top surface of filter inserts using cotton swabs. Cells on the bottom surface were then stained with Diff Quick stain (Dade Behring, Newark, DE) and cells in 5 randomly picked fields (at 40x magnification) were enumerated under a light microscope. All assays were carried out in triplicate and repeated three times. Cell migration was assayed as described for invasion assays but using Boyden chambers with uncoated filters (Becton Dickinson Biosciences, Bedford, MA).

Statistical analysis

For analysis of Matrigel invasion and gelatin degradation, differences were analyzed using a two-tailed student *t*-test with assumed unequal variance. For matrix-degradation difference between LAMP-1 positive and negative rosettes, Chi square test is used to analyze the data. Asterisks in figures represent a *P* value <0.01.

RESULTS

In this study, we used the classical model of podosome induced by v-Src in NIH3T3 cells. As expected (2), abundant actin dots and rosettes were observed in v-Src-transformed cells while these structures were absent in cells transduced with vector alone (Fig. S1A,B). These actin-structures were co-localized with focal loss of extracellular gelatin and the podosome markers (34) including phospho-tyrosine, cortactin, and vinculin (Fig. S1C). Thus, these actin-structures are bona fide podosomes.

Cysteine protease inhibitors reduce matrix degradation and invasion *in vitro*

We first investigated whether chemical inhibitors of cysteine proteases affected the degradation of labeled extracellular gelatin. Notably, treatment of v-Src-transformed cells with a cell-permeant (E64d) or a cell non-permeant (E64c) pan-cysteine protease inhibitor strongly blocked the degradation of labeled gelatin (Fig. 1A and B). Of the 11 cysteine cathepsins in lysosomes, cathepsins B's link to tumor invasion is most firmly established [reviewed in (23)]. Indeed, a cathepsin B-selective inhibitor CA074 and its cell-permeant but less selective form CA074Me both reduced the level of gelatin degradation (Fig. 1A and B). The pan-MMP inhibitor GM6001, used as a control, almost completely blocked the focal degradation of labeled gelatin by v-Src-transformed cells (Fig. 1A and B). These analyses suggested that, in addition to MMPs, cysteine cathepsins, and more specifically cathepsin B, are involved in matrix degradation at podosomes. In addition, we found that these enzymatic inhibitors of cysteine cathepsins inhibited the ability of v-Src-transformed cells to invade through Matrigel (Fig. 1C). shRNA-mediated knockdown of cathepsin B reduces the matrix degradation and invasion of v-Src NIH3T3 cells

Next, we used the shRNA-mediated knockdown as a complementary approach to further assess the role for cathepsin B in podosome function. Lentiviral vector control shRNAs and two shRNAs targeting cathepsin B were used to generate stably transduced cell lines. Immunoblotting using cathepsin B antibody revealed a band around 32 KD, corresponding to the mature single-chain cathepsin B (35). The levels of cathepsin B was reduced in cells transduced with two cathepsin B shRNAs, especially by number 2 shRNA (Fig. 2A). Compared with cells transduced with control vector, cathepsins B depleted v-Src-transformed cells also were less effective in digesting labeled extracellular gelatin and invading through a layer of Matrigel (Fig.2 B, C, D). Interestingly, the reduction in matrix-degradation and in vitro invasion assay correlated with the level of depletion in the two cathepsin B shRNA transduced cells.

The presence of LAMP-1 in podosome rosettes correlates with extensive extracellular gelatin degradation

These data prompt us to test whether lysosomes are localized at podosomes. Confocal immunostaining revealed that the lysosomal marker protein LAMP-1 was often detected in the vicinity of podosomes. Specifically, LAMP-1 was localized inside of some podosome rosettes (Fig. 3A, right panel and 3D). There were rosettes devoid of LAMP-1, which were generally smaller compared with those containing LAMP-1. To assess whether there was a size difference between rosettes with or without LAMP-1, we measured the diameters of podosomes in several randomly chosen fields. The average diameter of actin rosettes containing LAMP-1 were 6.6 μm whereas those without LAMP-1 were 2.72 μm in diameter (Fig. 3B). Furthermore, more than 65 percent of rosettes without LAMP-1 (23 out of 35) had limited gelatin-degradation which looked like a ring just underneath the actin rosette. In contrast, more than 83 percent of rosettes containing LAMP-1 (15 out of 18) had extensive internal gelatin-degradation which looked like a hole (Fig.3A and C). The differences in diameters and extent of matrix-degradation between rosettes with or without LAMP-1 were statistically significant.

Three dimensional localization of LAMP-1 in podosome rosette using confocal z-sectioning

The localization of LAMP-1 in podosomes could be a fortuitous co-incidence which may have no contact with the extracellular matrix. To address this question, we took serial confocal pictures along the z-axis and examined the localization of LAMP-1 in relation with gelatin-matrix in three dimensions. At degradation foci, LAMP-1 staining was found to be protruding into the matrix flanked by actin-ring of podosome rosettes. Moreover, residual extracellular matrix in the center of rosettes was found to be embedded in LAMP-1 positive vesicles (Fig. 3D). In contrast, those LAMP-1 positive vesicles found well above the extracellular matrix did not correspond to any gelatin-degradation foci (Fig.3D). The spatial proximity between

lysosome and eroding matrix suggest that lysosomes directly participate in the degradation of extracellular matrix at podosomes.

Time-lapse image analysis of the interaction between podosomes and lysosomes

Previously, lysosomes close to podosomes were thought to come from endosomes following the internalization of digested extracellular matrix components (36). This prompted us to perform time-lapse confocal microscopy to observe the dynamic interaction between podosomes and lysosomes. v-Src transformed NIH3T3 cells were transiently transfected with CFP-β-actin to visualize podosomes, which had been used to monitor the dynamics of podosomes (11). To visualize lysosomal vesicles in live cells, we loaded CFP-β-actin expressing v-Src NIH3T3 cells with a cell-permeant cathepsin B-selective crystal violet conjugated cathepsin B substrate $(RR)_2$ (Fig.4A and Supplemental movie#1) or lysotracker (Fig.4B and Supplemental movie#2). Most lysosomal vesicles and podosomes were distinct from each other (Fig.4). However, some lysosomal vesicles moved towards adjacent podosomes and remained associated with them for a few minutes. Later, these lysosomes disappeared while most lysosomal vesicles that did not interact with podosomes remained intact. Interestingly, some lysosomal vesicles also appeared to move out of podosomes (Fig. 4A and Supplemental movie#1). In contrast, the mitochondrial tracker-positive organelles were not found to interact with podosomes (Fig.S2).

Agents that alter lysosomal traffic promote podosome formation and matrix degradation

The results presented above suggested that lysosomal cysteine cathepsins may be recruited to podosomes to participate in matrix-degradation. Indeed, enhancing the secretion of lysosomes by calcium influx promotes podosome-formation in p61hck-expressing cells (31). Bafilomycin A1, an inhibitor of vacuolar H^+-ATPase (37), is known to inhibit the acidification of lysosomes and promote the secretion of lysosomal enzymes (38,39). This prompted us to test whether agents that alter the trafficking of lysosomes might affect podosome formation and matrix-degradation. We found that Bafilomycin A1 dramatically increased the gelatin-matrix degradation (Fig. 5) at concentrations as low as 5 nM. Notably, the percentage of cells with podosomes increased from approximately 50% to 90% (Fig. 5B) as did the number of podosomes in each cells (Fig.5A). Similar effects were obtained when cells were treated with other lysosomal alkalinizers, NH_4Cl or chloroquine (Fig. 5A and B).

The Bafilomycin A1-promoted degradation of extracellular gelatin was abrogated by pan-MMP inhibitor GM6001 or cysteine cathespin protease inhibitors including E64c, E64d, CA074, and CA074Me (Fig. 5C). Furthermore, depletion of cathepsin B effectively reduced the matrix degradation enhanced by Bafilomycin A1 treatment (Fig. 5D). These data suggest that both MMPs and lysosome-derived cysteine cathepsins such as cathepsin B are involved in lysosomal alkalinizer induced matrix degradation.

Bafilomycin A1 induces lysosome-associated podosome-like structures

The increase in podosome formation prompted us to investigate the effect of Bafilomycin A1 on dynamics of podosomes and lysosomes by live cell confocal microscope. Contrary to our expectation that Bafilomycin A1 would induce recruitment of lysosomes to pre-existing podosomes, we observed that pre-existing podosomes disappeared less than 5 minutes after Bafilomycin A1treatment (Fig.6A and supplemental movie #3). In contrast, the majority of podosomes were relatively stable in untreated cells for up to 10 minutes (Fig.6B), consisting with previous estimates of podosome half-lives ranging from 30 minutes to hours (11). After the dissolution of pre-existing podosomes, we observed that some lysosomal vesicles disappeared followed by the formation of actin-structures at the approximate same sites where lysosomal vesicles vanished. Meanwhile, many actin-structures appeared close to one end of

lysosomal vesicles (Fig.6A, C), which continued to moved with associated lysosomal vesicles up to 90 minutes after Bafilomycin A1 stimulation (Supplemental movie#3).

To characterize these Bafilomycin A1 induced actin-structures, we stained cells with phalloidin and antibodies against LAMP-1 and podosome markers phospho-tyrosine and cortactin respectively. Confocal microscopy revealed that these lysosome-associated actin-structures were positive for phospho-tyrosine and cortactin (Fig. S3). Thus, these actin-structures shared some characteristics of podosomes.

DISCUSSION

Experimental and clinical studies have established that lysosomal cysteine cathepsins such as cathepsin B contribute to tumor cell proliferation, angiogenesis, invasion and metastasis (16–19). Cysteine cathepsins achieve this through cleavage of cell adhesion molecules (19) and extracellular matrix components (40), and through the activation of other classes of proteases (41,42). However, the precise location and functional mechanism of pericellular cysteine cathepsins in these processes have not been fully elucidated. Here, we show that cathepsin B-positive lysosomal vesicles moved to podosomes and disappeared at podosomes (Fig.4), which most likely were the result of fusion between lysosomes and plasma membreane at podosomes. Using Z-sectioning and three-dimensional reconstitution, we also showed that lysosomes are in direct contact with matrix (Fig.3D) at podosomes. Importantly, the presence of lysosomal marker LAMP-1 inside podosome rosettes correlates with more extensive gelatin-matrix degradation, suggesting that the interaction is of functional significance. Taken together, our results suggest that lysosomal cysteine cathepsins may mediate matrix-digestion and cancer invasion through podosomes.

Essentially complete inhibition of the extracellular matrix-degradation by general inhibitors of either MMPs or the cysteine cathepsin family (Fig.1 and Fig.5) suggests that MMPs and cysteine cathepsins function in an inter-dependent manner. Most proteases, typically secreted in inactive pro-enzyme forms, are tightly regulated via endogenous inhibitors and self inactivation. Cathepsin B is known to promote the degradation of the endogenous MMP inhibitors TIMP-1 and TIMP-2 (43). In addition, extracellular cathepsins B can generate active urokinase-type plasminogen activator (uPA) (42), which in turn can activate pro-cathepsin B to form a positive feedback loop (44). uPA, likely located at podosomes via its receptor uPAR (24), can activate several types of MMPs by generating active plasmin (41,42). It is conceivable that a protease cascade of cathepsin B/uPA/plasmin/MMP may be initiated at podosomes, which are enriched with multiple proteases of the cascade.

A number of studies have linked the invasive and metastatic properties of tumor cells with an acidic extracellular environment (45), which in turn leads to secretion of lysosomal enzymes (46,47). The effects of Bafilomycin A1, ammonium chloride, and chloroquine on trafficking of lysosomal enzymes might mimic the lysosomal acidification defect found in some tumor cells (35,48). Recently, it was suggested that formation of invadopodia could be regulated by an acidic tumor environment and activation of a tumor-associated Na^+/H^+ exchanger NHE1 (45). Thus, our observation that disruption of normal lysosomal trafficking induces the assembly of podosomes may offer new insights into the mechanism of tumor invasion.

Several observations made here confirmed and extended the previous finding of a functional connection between lysosomes and podosomes (30–32). First, we show that lysosomes, together with lysosomal membrane proteins and enzymes such as LAMP-1 and cathepsin B, traffick to podosomes in a way similar to that of osteoclasts (26–29). Secondly, we showed here that agents that impair lysosomal function increased podosome formation and podosome-mediated matrix-degradation. The increase in podosome formation may be due to the increase

in the level of active Src (49 and our unpublished data) by lysotrophic agents. Furthermore, Bafilomycin A1 induced actin structures resemble those induced by p61hck (50) in that they are both associated with lysosomes. These data raise several interesting questions: Are Src family kinases that induce podosomes come from lysosomes? What is the relationship between podosome and these lysosome-associated actin structures? Answers to these questions may help shed light on the biogenesis of podosome.

In summary, our present study using v-Src transformed fibroblasts suggests a role for lysosomes in the function of podosomes by releasing cysteine cathepsin B for matrix-degradation. These data also suggest that altered trafficking of lysosomes may facilitate the metastatic behavior of cancer cells by modulating formation and function of podosomes.

Supplementary Material

Refer to Web version on PubMed Central for supplementary material.

Acknowledgments

References

1. Linder S, Aepfelbacher M. Podosomes: adhesion hot-spots of invasive cells. Trends Cell Biol 2003;13:376–85. [PubMed: 12837608]

2. Chen WT. Proteolytic activity of specialized surface protrusions formed at rosette contact sites of transformed cells. J Exp Zool 1989;251:167–85. [PubMed: 2549171]

3. Nakahara H, Nomizu M, Akiyama SK, Yamada Y, Yeh Y, Chen WT. A mechanism for regulation of melanoma invasion. Ligation of alpha6beta1 integrin by laminin G peptides. J Biol Chem 1996;271:27221–4. [PubMed: 8910291]

4. Kelly T, Yan Y, Osborne RL, et al. Proteolysis of extracellular matrix by invadopodia facilitates human breast cancer cell invasion and is mediated by matrix metalloproteinases. Clin Exp Metastasis 1998;16:501–12. [PubMed: 9872598]

5. Weaver AM. Invadopodia: specialized cell structures for cancer invasion. Clin Exp Metastasis 2006;23:97–105. [PubMed: 16830222]

6. Gimona M, Buccione R. Adhesions that mediate invasion. Int J Biochem Cell Biol 2006;38:1875–92. [PubMed: 16790362]

7. Linder S. The matrix corroded: podosomes and invadopodia in extracellular matrix degradation. Trends Cell Biol 2007;17:107–17. [PubMed: 17275303]

8. Linder S, Nelson D, Weiss M, Aepfelbacher M. Wiskott-Aldrich syndrome protein regulates podosomes in primary human macrophages. Proc Natl Acad Sci U S A 1999;96:9648–53. [PubMed: 10449748]

9. Berdeaux RL, Diaz B, Kim L, Martin GS. Active Rho is localized to podosomes induced by oncogenic Src and is required for their assembly and function. J Cell Biol 2004;166:317–23. [PubMed: 15289494]

10. Tehrani S, Faccio R, Chandrasekar I, Ross FP, Cooper JA. Cortactin has an essential and specific role in osteoclast actin assembly. Mol Biol Cell 2006;17:2882–95. [PubMed: 16611741]

11. Yamaguchi H, Lorenz M, Kempiak S, et al. Molecular mechanisms of invadopodium formation: the role of the N-WASP-Arp2/3 complex pathway and cofilin. J Cell Biol 2005;168:441–52. [PubMed: 15684033]

12. Gatesman A, Walker VG, Baisden JM, Weed SA, Flynn DC. Protein kinase Calpha activates c-Src and induces podosome formation via AFAP-110. Mol Cell Biol 2004;24:7578–97. [PubMed: 15314167]

13. Seals DF, Azucena EF Jr, Pass I, et al. The adaptor protein Tks5/Fish is required for podosome formation and function, and for the protease-driven invasion of cancer cells. Cancer Cell 2005;7:155–65. [PubMed: 15710328]

14. Freije JM, Balbin M, Pendas AM, Sánchez LM, Puente XS, López-Otín C. Matrix metalloproteinases and tumor progression. Adv Exp Med Biol 2003;532:91–107. [PubMed: 12908552]

15. Bauvois B. Transmembrane proteases in cell growth and invasion: new contributors to angiogenesis? Oncogene 2004;23:317–29. [PubMed: 14724562]

16. Joyce JA, Hanahan D. Multiple roles for cysteine cathepsins in cancer. Cell Cycle 2004;3:1516–619. [PubMed: 15539953]

17. Mohamed MM, Sloane BF. Cysteine cathepsins: multifunctional enzymes in cancer. Nat Rev Cancer 2006;6:764–75. [PubMed: 16990854]

18. Jedeszko C, Sloane BF. Cysteine cathepsins in human cancer. Biol Chem 2004;385:1017–27. [PubMed: 15576321]

19. Gocheva V, Zeng W, Ke D, et al. Distinct roles for cysteine cathepsin genes in multistage tumorigenesis. Genes Dev 2006;20:543–56. [PubMed: 16481467]

20. Monsky WL, Kelly T, Lin CY, et al. Binding and localization of M(r) 72,000 matrix metalloproteinase at cell surface invadopodia. Cancer Res 1993;53:3159–64. [PubMed: 8391388]

21. Nakahara H, Howard L, Thompson EW, et al. Transmembrane/cytoplasmic domain-mediated membrane type 1-matrix metalloprotease docking to invadopodia is required for cell invasion. Proc Natl Acad Sci U S A 1997;94:7959–64. [PubMed: 9223295]

22. Monsky WL, Lin CY, Aoyama A, et al. A potential marker protease of invasiveness, seprase, is localized on invadopodia of human malignant melanoma cells. Cancer Res 1994;54:5702–10. [PubMed: 7923219]

23. Ghersi G, Zhao Q, Salamone M, Yeh Y, Zucker S, Chen WT. The protease complex consisting of dipeptidyl peptidase IV and seprase plays a role in the migration and invasion of human endothelial cells in collagenous matrices. Cancer Res 2006;66:4652–61. [PubMed: 16651416]

24. Artym VV, Kindzelskii AL, Chen WT, Petty HR. Molecular proximity of seprase and the urokinase-type plasminogen activator receptor on malignant melanoma cell membranes: dependence on beta1 integrins and the cytoskeleton. Carcinogenesis 2002;23:1593–601. [PubMed: 12376466]

25. Saftig P, Hunziker E, Wehmeyer O, et al. Impaired osteoclastic bone resorption leads to osteopetrosis in cathepsin-K-deficient mice. Proc Natl Acad Sci U S A 1998;95:13453–8. [PubMed: 9811821]

26. Zhao H, Laitala-Leinonen T, Parikka V, Vaananen HK. Downregulation of small GTPase Rab7 impairs osteoclast polarization and bone resorption. J Biol Chem 2001;276:39295–302. [PubMed: 11514537]

27. Zhao H, Ettala O, Vaananen HK. Intracellular membrane trafficking pathways in bone-resorbing osteoclasts revealed by cloning and subcellular localization studies of small GTP-binding rab proteins. Biochem Biophys Res Commun 2002;293:1060–5. [PubMed: 12051767]

28. Mulari MT, Zhao H, Lakkakorpi PT, Vaananen HK. Osteoclast ruffled border has distinct subdomains for secretion and degraded matrix uptake. Traffic 2003;4:113–25. [PubMed: 12559037]

29. Blair HC, Teitelbaum SL, Ghiselli R, Gluck S. Osteoclastic bone resorption by a polarized vacuolar proton pump. Science 1989;245:855–7. [PubMed: 2528207]

30. Carreno S, Gouze ME, Schaak S, Emorine LJ, Maridonneau-Parini I. Lack of palmitoylation redirects p59Hck from the plasma membrane to p61Hck-positive lysosomes. J Biol Chem 2000;275:36223–9. [PubMed: 10967098]

31. Cougoule C, Carreno S, Castandet J, et al. Activation of the lysosome-associated p61Hck isoform triggers the biogenesis of podosomes. Traffic 2005;6:682–94. [PubMed: 15998323]

32. Kasahara K, Nakayama Y, Kihara A, et al. Rapid trafficking of c-Src, a non-palmitoylated Src-family kinase, between the plasma membrane and late endosomes/lysosomes. Exp Cell Res 2007;313:2651–66. [PubMed: 17537435]

33. Moin K, Day NA, Sameni M, Hasnain S, Hirama T, Sloane BF. Human tumour cathepsin B. Comparison with normal liver cathepsin B. Biochem J 1992;285:427–34. [PubMed: 1637335]

34. Mueller SC, Yeh Y, Chen WT. Tyrosine phosphorylation of membrane proteins mediates cellular invasion by transformed cells. J Cell Biol 1992;119:1309–25. [PubMed: 1447304]

35. Lorenzo K, Ton P, Clark JL, Coulibaly S, Mach L. Invasive properties of murine squamous carcinoma cells: secretion of matrix-degrading cathepsins is attributable to a deficiency in the mannose 6-phosphate/insulin-like growth factor II receptor. Cancer Res 2000;60:4070–6. [PubMed: 10945612]

36. Coopman P, Do M, Thompson E, Mueller SC. H Phagocytosis of cross-linked gelatin matrix by human breast carcinoma cells correlates with their invasive capacity. Clin Cancer ReHs 1998;4:507–15.

37. Yoshimori T, Yamamoto A, Moriyama Y, Futai M, Tashiro Y. Bafilomycin A1, a specific inhibitor of vacuolar-type H(+)-ATPase, inhibits acidification and protein degradation in lysosomes of cultured cells. J Biol Chem 1991;266:17707–12. [PubMed: 1832676]

38. Oda K, Nishimura Y, Ikehara Y, Kato K. Bafilomycin A1 inhibits the targeting of lysosomal acid hydrolases in cultured hepatocytes. Biochem Biophys Res Commun 1991;178:369–77. [PubMed: 2069575]

39. Tapper H, Sundler R. Bafilomycin A1 inhibits lysosomal, phagosomal, and plasma membrane H(+)-ATPase and induces lysosomal enzyme secretion in macrophages. J Cell Physiol 1995;163:137–44. [PubMed: 7896890]

40. Buck MR, Karustis DG, Day NA, Honn KV, Sloane BF. Degradation of extracellular-matrix proteins by human cathepsin B from normal and tumour tissues. Biochem J 1992;282:273–78. [PubMed: 1540143]

41. Kobayashi H, Schmitt M, Goretzki L, et al. Cathepsin B efficiently activates the soluble and the tumor cell receptor-bound form of the proenzyme urokinase-type plasminogen activator (Pro-uPA). J Biol Chem 1991;266:5147–52. [PubMed: 1900515]

42. Guo M, Mathieu PA, Linebaugh B, Sloane BF, Reiners JJ Jr. Phorbol ester activation of a proteolytic cascade capable of activating latent transforming growth factor-betaL a process initiated by the exocytosis of cathepsin B. J Biol Chem 2002;277:14829–37. [PubMed: 11815600]

43. Kostoulas G, Lang A, Nagase H, Baici A. Stimulation of angiogenesis through cathepsin B inactivation of the tissue inhibitors of matrix metalloproteinases. FEBS Lett 1999;455:286–90. [PubMed: 10437790]

44. Dalet-Fumeron V, Guinec N, Pagano M. In vitro activation of pro-cathepsin B by three serine proteinases: leucocyte elastase, cathepsin G, and the urokinase-type plasminogen activator. FEBS Lett 1993;332:251–4. [PubMed: 8405467]

45. Cardone RA, Casavola V, Reshkin SJ. The role of disturbed pH dynamics and the Na+/H+ exchanger in metastasis. Nat Rev Cancer 2005;5:786–95. [PubMed: 16175178]

46. Rofstad EK, Mathiesen B, Kindem K, Galappathi K. Acidic extracellular pH promotes experimental metastasis of human melanoma cells in athymic nude mice. Cancer Res 2006;66:6699–707. [PubMed: 16818644]

47. Glunde K, Guggino SE, Solaiyappan M, Pathak AP, Ichikawa Y, Bhujwalla ZM. Extracellular acidification alters lysosomal trafficking in human breast cancer cells. Neoplasia 2003;5:533–45. [PubMed: 14965446]

48. Rozhin J, Sameni M, Ziegler G, Sloane BF. Pericellular pH affects distribution and secretion of cathepsin B in malignant cells. Cancer Res 1994;54:6517–25. [PubMed: 7987851]

49. Kim M, Tezuka T, Tanaka K, Yamamoto T. Cbl-c suppresses v-Src-induced transformation through ubiquitin-dependent protein degradation. Oncogene 2004;23:1645–55. [PubMed: 14661060] Erratum in: Oncogene. 2004;23:7903-4

50. Vincent C, Maridonneau-Parini I, Le Clainche C, Gounon P, Labrousse A. Activation of p61Hck triggers WASp- and Arp2/3-dependent actin-comet tail biogenesis and accelerates lysosomes. J Biol Chem 2007;282:19565–74. [PubMed: 17500055]
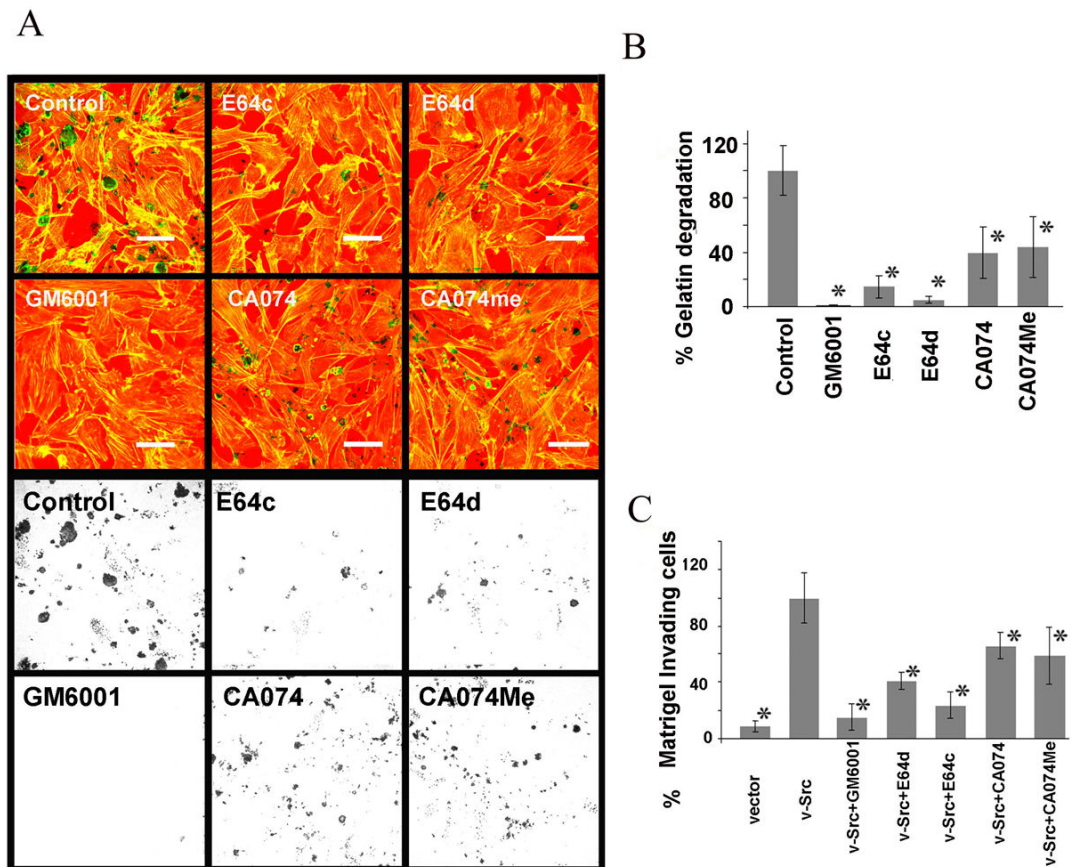
Fig. 1.
Cysteine cathepsin B inhibitors block matrix degradation and invasion by v-SrcNIH-3T3 cells.
A). v-Src NIH3T3 cells cultured on cy3-gelatin in the presence of DMSO (vehicle control), 10 μM GM6001, 50 μM E64c, 50 μM E64d, 10 μM CA074, or 10 μM CA074Me were stained for filamentous actin (F-actin) with Alexa 488-phalloidin (green). Scale bars, 20μm. B).The graph shows the percentage (± standard deviation (S.D.)) of gelatin-degradation in each condition compared with DMSO treated v-Src cells. C). v-Src NIH3T3 cells treated with DMSO, 10 μM GM6001, 50 μM E64c, 50 μM E64d, 10 μM CA074 or 10 μM CA074Me as well as untreated vector-transduced NIH3T3 cells were tested for their ability to invade through Matrigel in a Boyden chamber assay. The graph shows the percentage (± S.D.) of invaded cells compared with DMSO-treated v-Src cells. The asterisks* indicates statistically significant differences (*P*<0.01).
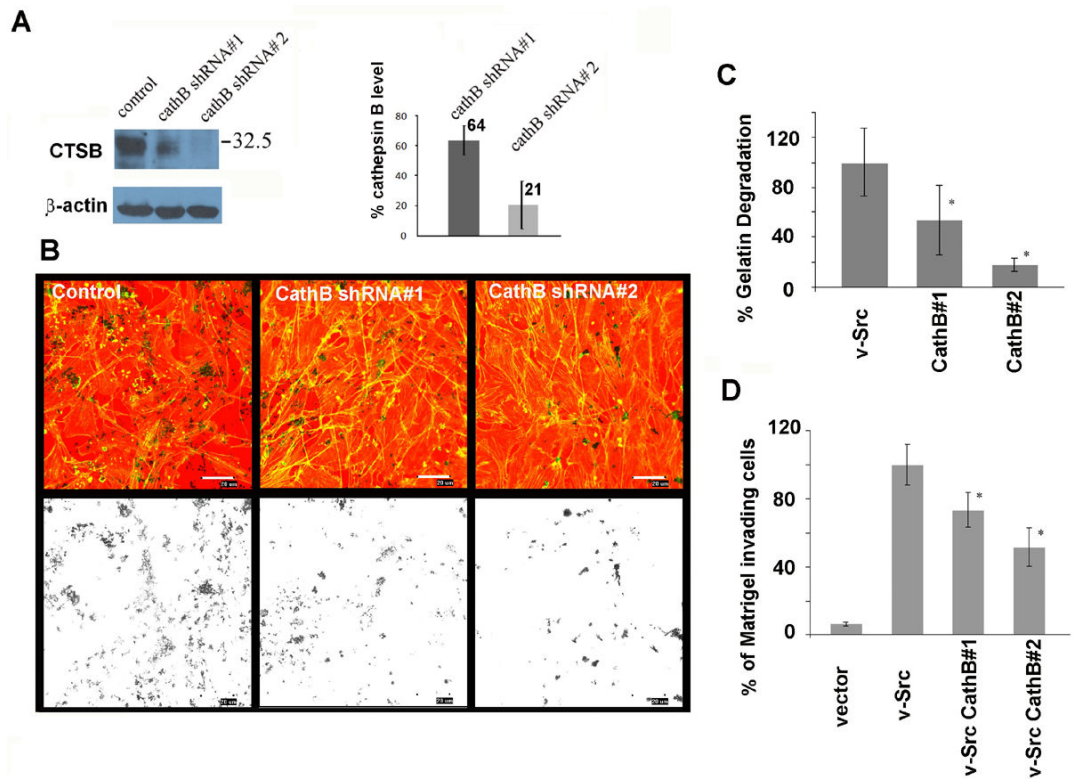
Fig. 2.
Cathepsin B depletion inhibits matrix degradation and invasion by v-Src NIH3T3 cells. A). Immunoblot analysis of cathepsin B (CTSB) and β-actin (as loading control) in v-Src NIH3T3 cells transduced with shRNAs against cathepsin B or control shRNA. The graph on the right shows percentage (± S.D.) of the cathepsin B level compared to control cells. B). Control cells and cathepsin B-depleted cells cultured on cy3-labeled gelatin (red)-coated coverslips were stained with Alexa 488-phalloidin (green). C).The graph shows the percentage (±S.D.) of gelatin-degradation compared with control v-Src cells. D). Control and cathepsin B depleted v-Src NIH3T3 cells and NIH3T3 cells were assessed for their ability to invade through Matrigel in a Boyden chamber assay. The graph shows the percentage (mean ± S.D.) of invaded cells compared with control v-Src cells. The asterisks* indicates statistically significant differences (*P*<0.01).
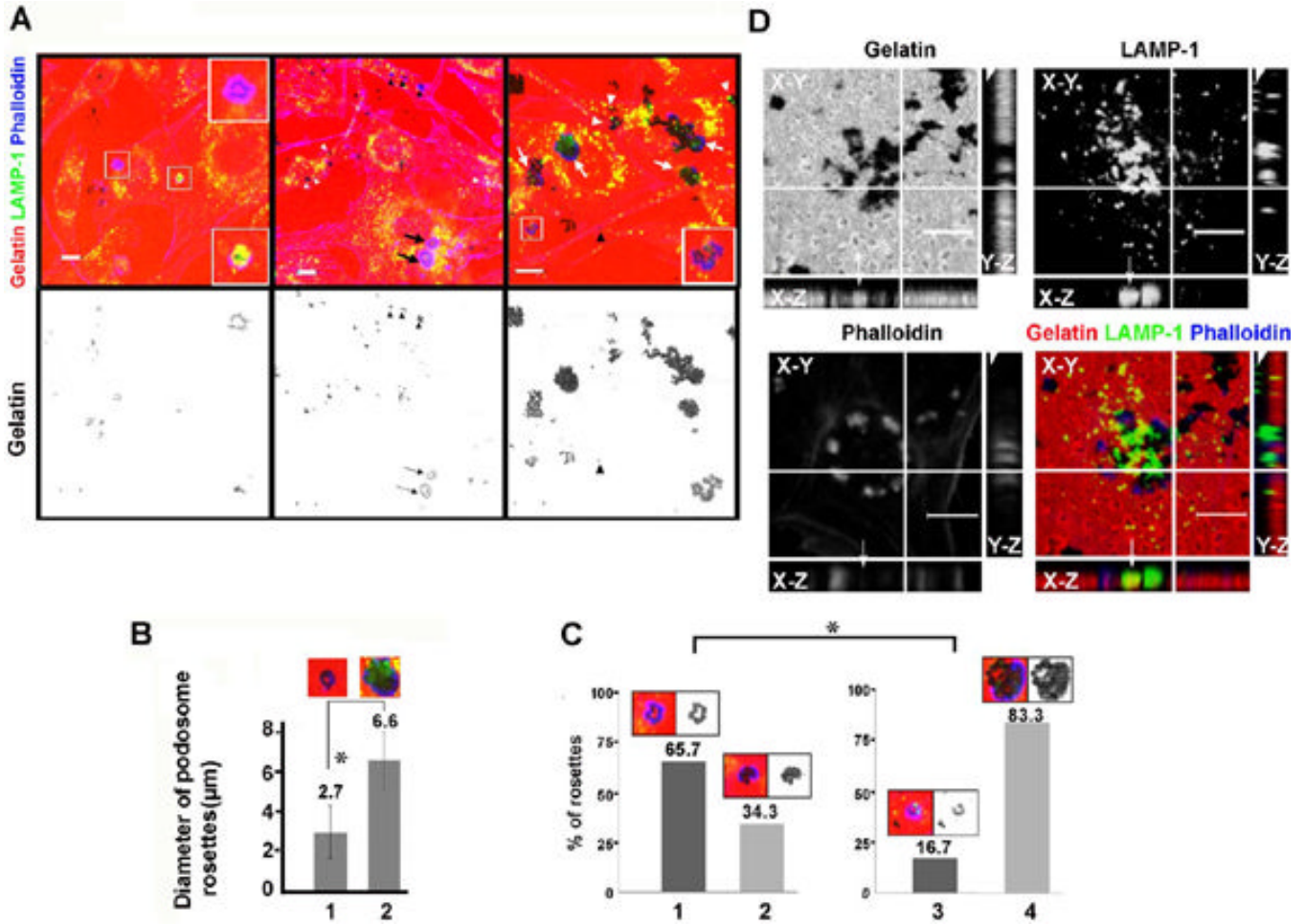
Fig. 3.
Podosome rosettes positive for lysosomal marker LAMP-1 are bigger and more active in matrix-degradation. A). Three fields of v-Src NIH-3T3 cells cultured on cy3-gelatin-coated (red) coverslips representing different types of podosome dots and rosettes. Cell were stained with an antibody against LAMP-1(green) and Alexa 647-labeled phalloidin for F-actin (blue). White and black arrowheads show gelatin-degradation foci co-localized with LAMP-1or podosome respectively. White arrows show rosettes with LAMP-1 inside. Black arrows show rosettes surrounded by LAMP-1. Scale bars: 10 μm. B). Difference in diameters of podosome rosettes without (column 1) and those with LAMP-1 (column 2) were significant (P<0.01 by T test). C). Gelatin-degradation patterns of LAMP-1 negative (left graph) rosettes and positive rosettes (right graph) are different (*P*<0.01 by Chi square test). 65.7% of LAMP-1 negative rosettes and 16.7% of LAMP-1 positive rosettes were ring-like (column1, 3 respectively) while 34.4% LAMP-1 negative and 83.3% LAMP-1 positive rosettes were hole-like (column2,4). The asterisks* indicates statistically significant differences. D). Three-dimensional localizations of LAMP-1, rosette, and matrix. Crosshair in XY section shows the locations of the XZ and YZ cross-sections. Cell is on top of matrix in XZ section. Cell is at left and matrix is on right in YZ section. Arrow shows LAMP-1 in close contact with gelatin matrix. Arrowhead in YZ section shows several lysosomal vesicles inside cells. Size bar: 5μm
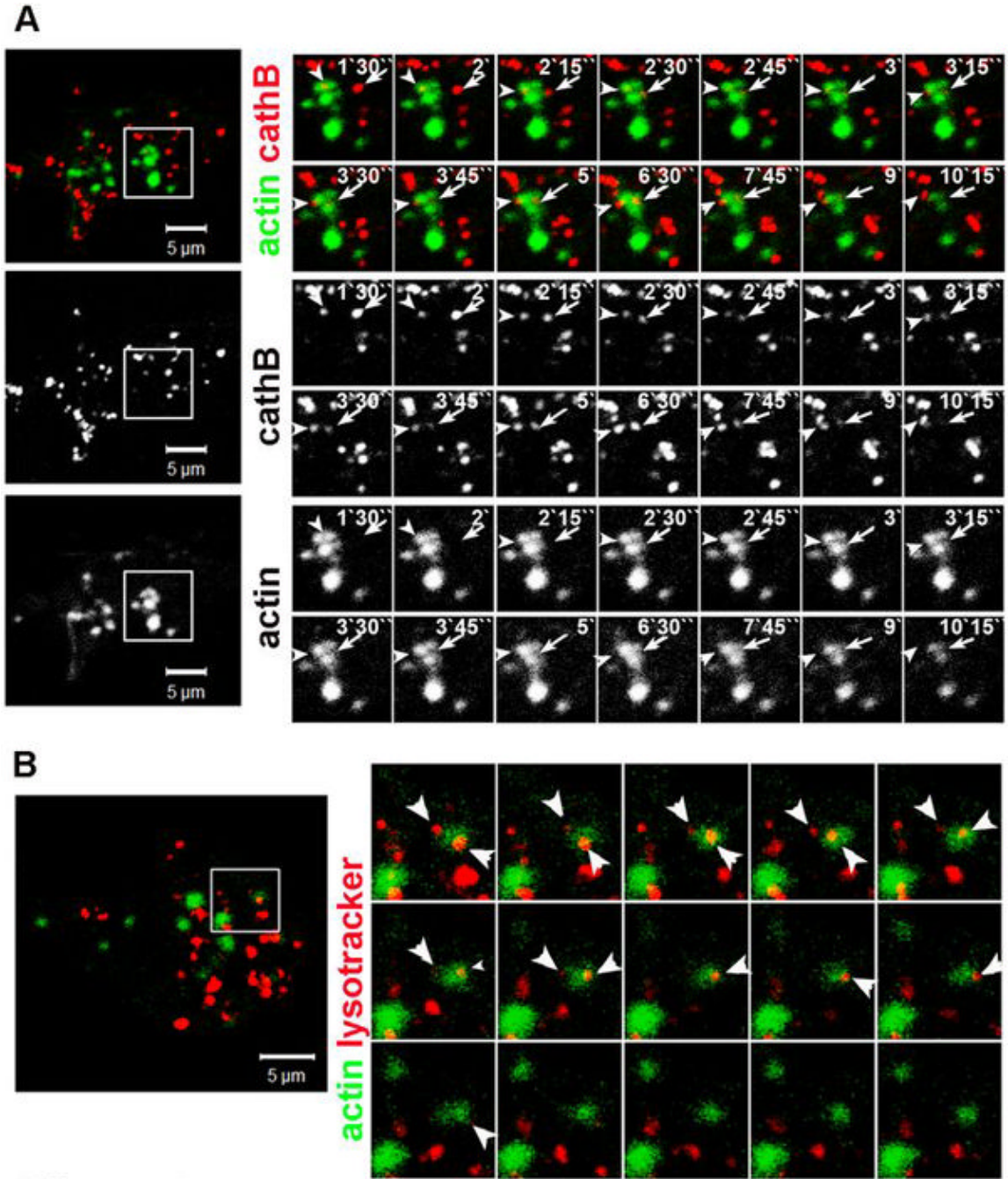
Fig. 4.
Dynamic interaction between lysosomes and podosomes in live cells.
Time-lapse image sequence of v-Src NIH3T3 cells expressing CFP-β-actin (green) loaded with crystal violet conjugated cathepsin B substrate (RR)$_2$ (A) or lysotracker (B). The large panels on the left show the whole cell at the begining of the video. A). Arrow shows a cathepsin B-positive lysosomal vesicle moved toward a podosome at 2 minutes 15 seconds and disappeared around 8 minutes later. Arrowhead shows that a cathepsin B-positive lysosomal vesicle located in podosome rosettes at the start but moved out of the podosome 9 minutes later. B). Arrowheads show two lysotracker-positive lysosomal vesicles approaching a podosome at 0 minutes and disappeared at the periphery of the podosome around 3 minutes later.
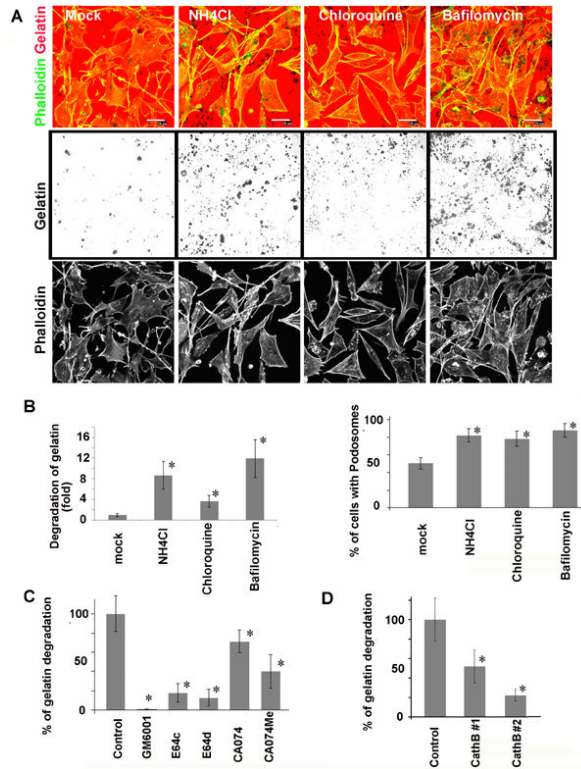
Fig. 5.
Agents that disrupt the pH gradient of lysosomes enhance the matrix degradation and podosome formation. A).v-Src NIH3T3 cells cultured on cy3-gelatin-coated (red) coverslips were mock-treated (0.1%DMSO) or treated with 5 mM NH$_4$Cl, 5 nM Bafilomycin A1, or 50 μM chloroquine for 8 hours. Cells were then stained with Alexa 488-phalloidin (green). B). The left graph shows the fold (±S.D.) of gelatin degradation compared with mock-treated v-Src NIH-3T3 cells (Left panel). The right graph shows the percentage of cells containing podosomes in each condition. C). v-Src NIH-3T3 cells were treated with 5 nM Bafilomycin A1 alone or in addition to 10 μM GM6001, 50 μM E64c, 50 μM E64d, 10 μM CA074, or 10 μM CA074Me. The graph shows the percentage (±S.D.) of gelatin-degradation in each conditions. D). The graph shows the percentage (±S.D.) of gelatin-degradation in control, cathepsin B- depleted v-Src-transformed NIH-3T3 cells treated with 5 nM Bafilomycin A1. The asterisks* indicates statistically significant differences ($P<0.01$).
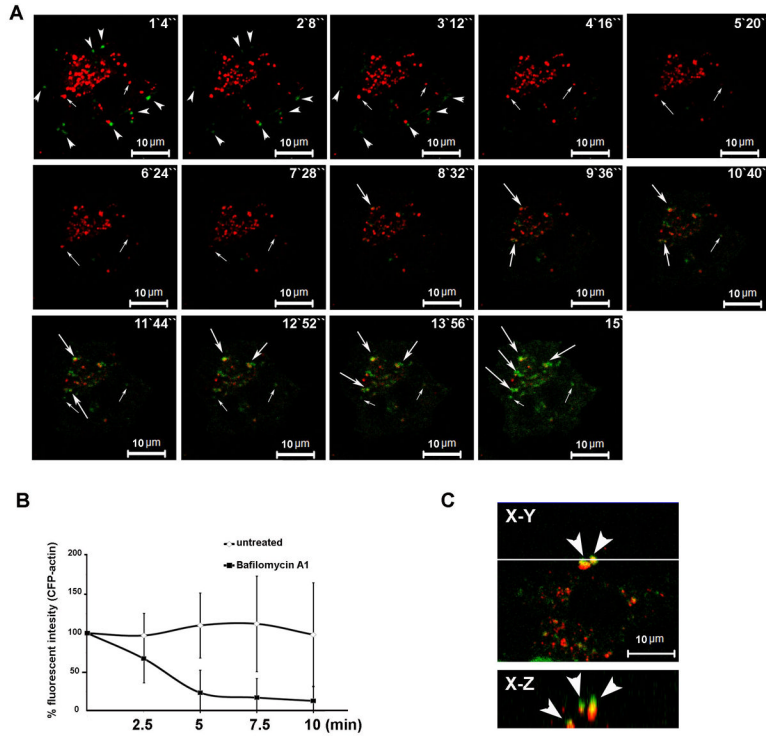
Fig. 6.
Bafilomycin induces lysosome-associated actin structures.

A). Time-lapse live-cell image sequence of v-Src NIH3T3 cells expressing CFP-β-actin (green) loaded with crystal violet-conjugated cathepsin B substrate $(RR)_2$ (red). Cells were then treatment with 20mM Bafilomycin A1. Frames were taken 64 seconds apart. Arrowhead shows that pre-existing podosome dots disappeared over time. Small arrow shows the loss of lysosome vesicles followed by the appearance of actin dots at the same sites. Big arrow shows lysosomal vesicles became associated with actin-rich structures after Bafilomycin A1 treatment. B). The change of β-actin intensities of podosome area in untreated (n=35) or Bafilomycin A1 treated (n=47) cells over 10 minutes. The difference between untreated and treated is statistically significant (p<0.001 after 2.5 minutes by T tests). C). Three dimensional localization ofBafilomycin A1 induced actin structures and lysotracker positive lysosomes in live cell. White line in XY panel shows the location of the XZ section. The bottom of XZ panel is close to the ventral side of plasma membrane.